Electric Power Systems Research 80 (2010) 345–353

Contents lists available at ScienceDirect

Electric Power Systems Research

journal homepage: www.elsevier.com/locate/epsr

DSTATCOM with Flywheel Energy Storage System for wind energy applications: Control design and simulation

G.O. Suvire*, P.E. Mercado

CONICET, Instituto de Energía Eléctrica, Universidad Nacional de San Juan, San Juan, Argentina

ARTICLE INFO

Article history:
Received 15 January 2009
Received in revised form
25 September 2009
Accepted 28 September 2009
Available online 29 October 2009

Keywords:
Dynamic modeling
DSTATCOM
Flywheel
Wind power

ABSTRACT

In this work, the use of a Distribution Static Synchronous Compensator (DSTATCOM) coupled with a Flywheel Energy Storage System (FESS) is proposed to mitigate problems introduced by wind generation in the electric system. A dynamic model of the DSTATCOM/FESS device is introduced and a multi-level control technique is proposed. This control technique presents one control mode for active power and two control modes for reactive power, power factor correction, and voltage control. Tests of dynamic response of the device are conducted, and performance characteristics are studied taking into consideration variations of power references. Moreover, the behaviour of the device is analyzed when combined with wind generation in the electric system. The results obtained demonstrate a good performance of the model developed and of the control technique proposed as well as a high effectiveness of the device to mitigate problems introduced by wind generation.

1. Introduction

Wind power generation is considered the most economic viable alternative within the portfolio of renewable energy resources. Among its main advantages are the large number of potential sites for plant installation and a rapidly evolving technology. However, the lack of controllability over the wind and the type of generation system used cause problems to the electric systems. Among such problems are those produced by wind power short-term fluctuations, e.g., in the power quality and in the dynamics of the system [1–5]. In addition, the reduced cost of power electronic devices as well as the breakthrough of new technologies in the field of electric energy storage makes it possible to incorporate this storage with electronic control into power systems [6–9]. These devices allow a dynamic control to be made of both voltage and flows of active and reactive power. Therefore, they offer a great potential in their use to mitigate problems introduced by wind generation.

Based on the results obtained by analyzing different selection criteria, a Distribution Static Synchronous Compensator (DSTATCOM) coupled with a Flywheel Energy Storage System (FESS) has been proposed as the most appropriate system for contributing to the smoothing of wind power short-term fluctuations [10]. A DSTATCOM is a fast-response, solid-state power controller that provides flexible voltage control at the point of connection to the utility distribution feeder for power quality improvements [11]. This device can exchange both active and reactive power if an energy storage system is included into the DC bus. FESSs store kinetic energy in a rotating mass, and they have been used as short-term energy storage devices. FESSs can be classified as low-speed flywheel (LS-FESS) and high-speed flywheel (HS-FESS). HS-FESSs are a newer technology and they provide better speeds of response, cycling characteristics and electric efficiencies than LS-FESS [9,12,13]. All these characteristics enable the HS-FESS (FESS from now on), working with a DSTATCOM device, to mitigate voltage fluctuations and to correct power fluctuations of a wind power system. With these aspects in mind, it turns necessary to ponder the information stemming from models that simulate the dynamic interaction between the DSTATCOM/FESS device and power systems with wind generation. Such models allow performing the necessary preliminary studies before connecting the DSTATCOM/FESS to the grid. Many solutions are proposed and studied in the literature to compensate wind power fluctuations using a flywheel energy storage device [14–17]. These solutions have been proposed mainly using LS-FESS and with simplified models of the device. The control design to interact with wind power generation is not explained in detail in the analyzed literature.

The aim of this paper is to present a detailed model and a multi-level control of a DSTATCOM controller coupled with FESS to improve the integration of wind generators (WGs) into a power system. A model of a DSTATCOM/FESS device is proposed with all its components represented in detail. The results obtained from the simulations of this model are compared with characteristic data of manufactures. Moreover, the complete control design for

* Corresponding author at: IEE-FI-UNSJ, Av. Lib. San Martín 1109 (Oeste), J5400ARL, Capital, San Juan, Argentina. Tel.: +54 264 4226444; fax: +54 264 4210299.
E-mail address: gsuvire@iee.unsj.edu.ar (G.O. Suvire).

0378-7796/$ – see front matter © 2009 Elsevier B.V. All rights reserved.
doi:10.1016/j.epsr.2009.09.020

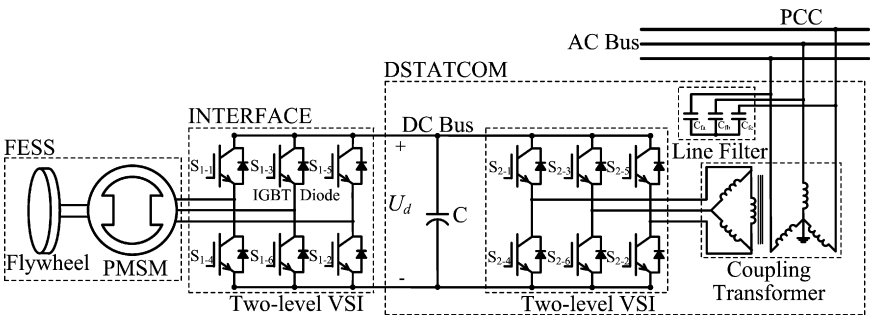

Fig. 1. Representation of the DSTATCOM/FESS controller.

this device is suggested. This control implements a new approach based on multi-level control technique. To mitigate wind power fluctuations, the control includes three modes of operation of the DSTATCOM/FESS device, namely, voltage control, power factor correction, and active power control. Validation of models and control schemes is carried out through simulations by using SimPowerSystems of SIMULINK/MATLAB™.

2. Modeling of the DSTATCOM/FESS

In order to study the dynamic performance of the DSTATCOM/FESS controller, a detailed model of the combined system is proposed that is depicted in Fig. 1. This model consists mainly of the DSTATCOM controller, the Interface converter and the FESS device.

The DSTATCOM and the Interface use two-level VSIs. The commutation valves used are Insulated Gate Bipolar Transistors (IGBT) with anti-parallel diodes. The VSIs are modeled with detailed blocks of the switches and diodes, incorporated into the simulation program. The technique of sinusoidal pulse width modulation (SPWM) is used to obtain a sinusoidal voltage waveform. In order to reduce the disturbance produced on the distribution system by the high-frequency switching harmonics generated by the SPWM control, a low pass sine wave filter is used.

The energy stored by a FESS is calculated by using Eq. (1).

$$\Delta E = \frac{J(\omega_{\max}^2 - \omega_{\min}^2)}{2} \tag{1}$$

where ΔE is the energy stored by the flywheel, ω_{max} and ω_{min} are, respectively, the maximum and minimum operation speed of the flywheel, and J is the moment of inertia of the flywheel.

The exchange of power between the flywheel and the Interface is made by using a Permanent Magnet Synchronous Machine (PMSM). The PMSM is modeled with a detailed block included in the simulation program and with parameters obtained from the manufacturer data sheets [13,18,19]. The flywheel is modeled as an additional mass coupled to the rotor shaft of the PMSM [20].

3. DSTATCOM/FESS control

The control proposed for the DSTATCOM/FESS device is divided into two parts, the DSTATCOM control and the FESS control. For each part, a multi-level control scheme is suggested. This scheme has its own control objectives for each level. In this way, a system of complex control is divided into several control levels, which are simpler to design [21,22]. Both parts of the multi-level control scheme, i.e., the DSTATCOM and the FESS, are divided into three quite distinct levels: external, middle and internal level, shown in simplified way in Fig. 2.

3.1. DSTATCOM control

Each control level of the DSTATCOM has certain functions. The external level is responsible for determining the active and reactive power exchange between the DSTATCOM and the utility system. The middle level control allows the expected output to dynamically track the reference values set by the external level. The internal level is responsible for generating the switching signals for the valves of the VSI of the DSTATCOM. The control algorithm of the DSTATCOM with all its parts in detail is shown in Fig. 3.

Control is performed with the synchronous-rotating dq reference frame. The coordinate system is defined with the d-axis always coincident with the instantaneous voltage vector ($u_d = |u|$, $u_q = 0$). Consequently, the d-axis current component contributes to the instantaneous active power and the q-axis current component represents the instantaneous reactive power.

3.2. External level control

The external level control scheme proposed (left side in Fig. 3) is designed for performing three major control objectives, namely, the voltage control mode (VCM), which is activated when switch S is in position a, the power factor control mode (PFCM), activated in position b, and the active power control mode (APCM), which is always activated.

The VCM consists in controlling the voltage at the PCC (Point of Common Coupling) of the DSTATCOM through the modulation of the reactive component of the output current. To this aim, the instantaneous voltage at the PCC (u_d) is computed by using a synchronous-rotating orthogonal reference frame and is then compared with a reference voltage (U_r). A voltage regulation droop (or

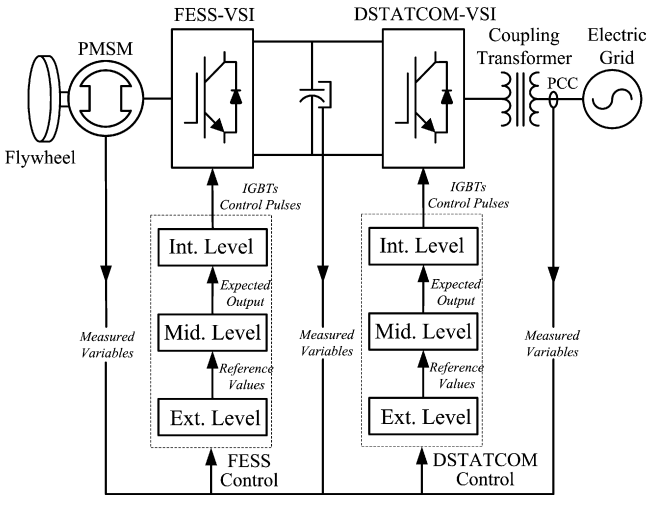

Fig. 2. Structure of the multi-level control of the DSTATCOM/FESS.

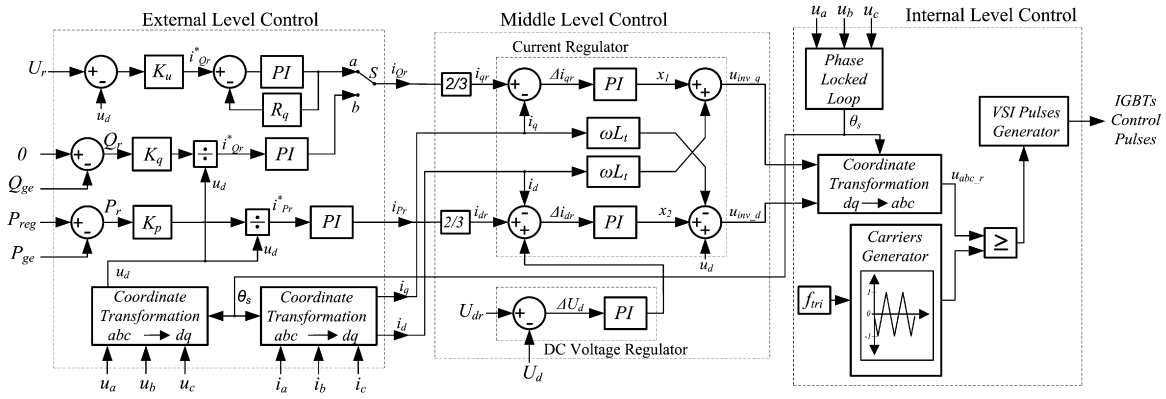

Fig. 3. Multi-level control scheme of the DSTATCOM device.

slope) R_q is included in order to allow the terminal voltage of the DSTATCOM to vary in proportion with the compensating reactive current.

In the PFCM, the reactive power reference (Q_r) is set to the measured value of the reactive power of wind generation (Q_{ge}). In this way, all the reactive power required by the WG is provided and thus the WG-DSTATCOM/FESS system is able to maintain the unity power factor. A standard PI compensator is included to eliminate the steady-state error in the reactive current reference computation.

The APCM allows controlling the active power exchanged with the electric system. The computation of the reference active power (P_r) depends on the active power value injected by the wind generation. This value is the difference between the regulation power desirable (P_{reg}) and the active power measured from the WG (P_{ge}). The P_{reg} is the active power that needs to be delivered to the electric system by the WG-DSTATCOM/FESS system. A standard PI compensator is also included to eliminate the steady-state error in the active current reference computation.

3.3. Middle level control

This block has two main parts, the DC voltage regulator and the current regulator. A functional simplified scheme of this control level is shown in the central part of Fig. 3.

The dynamic equations governing the power instantaneous transfer between the DSTATCOM and the electrical network are given by Eq. (2).

$$\frac{d}{dt}\begin{bmatrix} i_q \\ i_d \end{bmatrix} = \begin{bmatrix} -\omega & -R_t/L_t \\ -R_t/L_t & \omega \end{bmatrix}\begin{bmatrix} i_d \\ i_q \end{bmatrix} + \frac{1}{L_t}\begin{bmatrix} u_{inv\_q} \\ u_{inv\_d} - |u| \end{bmatrix} \tag{2}$$

where R_t and L_t are, respectively, the resistance and equivalent leakage inductance of the coupling transformer of the DSTATCOM.

A control methodology to obtain a decoupled control of the current components, i_d and i_q, is derived from Eq. (2). To achieve this objective, two appropriate control signals x_1 and x_2 are introduced. If $i_q R_t/L_t = x_1$ and $i_d R_t/L_t = x_2$, and Eq. (2) is worked and these variables introduced; then, Eq. (2) results in Eq. (3).

$$\frac{d}{dt}\begin{bmatrix} i_q \\ i_d \end{bmatrix} = \begin{bmatrix} 0 & -R_t/L_t \\ -R_t/L_t & 0 \end{bmatrix}\begin{bmatrix} i_d \\ i_q \end{bmatrix} + \begin{bmatrix} x_1 \\ x_2 \end{bmatrix} \tag{3}$$

As can be noticed from the equation above, i_d and i_q respectively respond to x_1 and x_2 with no cross-coupling. Conventional PI controllers with proper feedback from the DSTATCOM/FESS output current component are used to obtain the decoupling condition.

In addition, the AC and DC sides of the DSTATCOM are related by the power balance between the input and the output as described by Eq. (4).

$$P_{AC} = (u_{inv\_d} i_d + u_{inv\_q} i_q)\frac{3}{2} = \frac{-CU_d dU_d}{dt} - \frac{U_d^2}{R_{pd}} = P_{DC} \tag{4}$$

where R_{pd} is the loss resistance of the VSI and U_d is the DC voltage. Considering $u_{inv\_d} = k_{inv}\cos\alpha U_d$ and $u_{inv\_q} = k_{inv}\sin\alpha U_d$, with $k_{inv} = m_a a_t/2$, (m_a is the modulation index and $a_t = n_1/n_2$ the voltage ratio of the coupling transformer) and α is the phase-shift between the converter output voltage and the grid AC voltage; Eq. (4) may be rewritten as:

$$\frac{dU_d}{dt} = \frac{-3k_{inv}(i_d\ \cos\alpha + i_q\ \sin\alpha)}{2C} - \frac{U_d}{CR_{pd}} \tag{5}$$

Another PI compensator which allows eliminating the steady-state voltage variations at the DC bus is used by forcing a small active power exchange with the electric grid.

3.4. Internal level control

A basic scheme of the internal level control of the DSTATCOM is shown on the right side of Fig. 3. This level is mainly composed of a line synchronization module and a three-phase PWM firing pulses generator for the DSTATCOM-VSI. The line synchronization module consists mainly of a phase locked loop (PLL) [23]. The three-phase firing pulses generator produces both a frequency triangular wave (f_{tri}) and the firing pulses for each IGBT of the VSI by comparing this triangular wave with the desired reference three-phase voltage, u_{abc_r}.

3.5. FESS control

The FESS control is carried out through the control of the Interface-VSI. By establishing a three-phase voltage of controllable amplitude and phase with the VSI, the PMSM can work as a motor storing energy or as generator delivering energy. In a way similar to the DSTATCOM control, each control level has to perform certain functions. The external level is responsible for determining the power exchange between the DC bus of the DSTATCOM and the FESS so as to fulfil the power requirements imposed by the DSTATCOM. The middle and internal levels basically have the same functions as the middle and internal control levels of the DSTATCOM, respectively. The control algorithm of the FESS is shown in Fig. 4.

3.6. External level control

The external level control of the FESS is shown in simplified way on the left side of Fig. 4. In this control scheme, the reference current

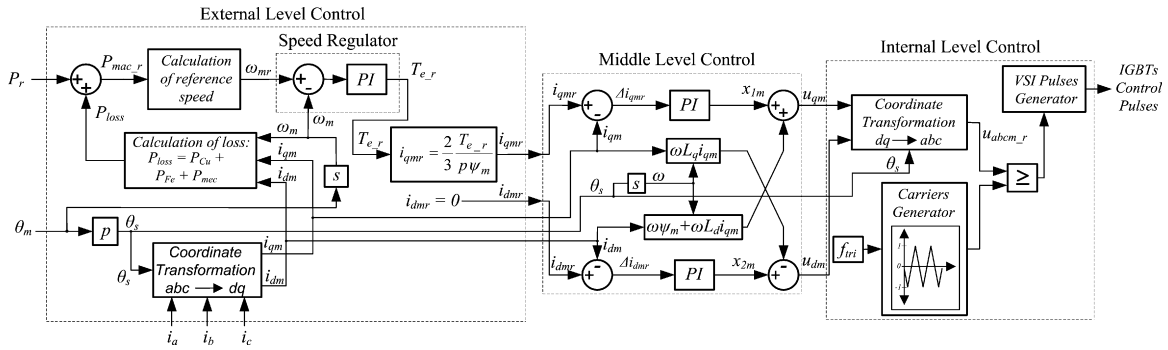

Fig. 4. Multi-level control scheme of the FESS.

i_{qmr} is computed from the torque of the PMSM by using Eq. (6), and the reference current i_{dmr} is set to zero. In this way, a maximum efficiency of the PMSM is obtained [24].

$$T_{e\_r} = \frac{3p\psi_m i_{qmr}}{2} \tag{6}$$

where T_{e_r} is the electromagnetic torque of the machine, p the number of pairs of poles and ψ_m the magnetic flux.

The reference torque is calculated through a speed regulator which adjusts the actual speed of the machine (ω_m) to the reference speed of the machine (ω_{mr}) by using a PI controller. The reference speed is computed from the reference power of the machine, P_{mac_r}, (the power that is to be stored or delivered by the flywheel) using Eq. (7).

$$P_{mac\_r} = \frac{d(J\omega_{mr}^2/2)}{dt} \tag{7}$$

The reference power of the machine is calculated by summing up the reference power of the DSTATCOM/FESS (P_r) and the power losses of the machine (P_{loss}). The losses of the machine are computed by summing up the copper losses (P_{Cu}) the iron losses (P_{Fe}) and the mechanical losses (P_{mec}) [25].

3.7. Middle level control

A functional simplified scheme of middle level control is shown in the central part of Fig. 4. This level is basically composed of a current regulator. The control is made by using vector control; the main characteristic of this control is the synchronization of the stator flux with the rotor. The currents in the d and q axes are regulated separately. The control scheme is similar to the middle level control of the DSTATCOM, except that the synchronism angle to make the coordinate transformation, θs, is computed in a different way. In this case, the angle is obtained by measuring the position angle of the machine (θ_m) and multiplying by the number of pairs of poles.

3.8. Internal level control

A basic scheme of the internal level control of the FESS is shown on the right side of Fig. 4. This control level is quite similar to that of the internal level control of the DSTATCOM except that it does not have the phase locked loop block due to the fact that the angle θs is obtained through measurement as mentioned before.

4. Test system

The test power system used to study the dynamic performance of the DSTATCOM/FESS device proposed is shown in Fig. 5 as a single line diagram. This sub-transmission system operates at 13.8 kV/50 Hz and implements a dynamically modeled wind generator linked to a bulk power system represented by an infinite bus type.

The WG (rated power: 750 kW) uses an induction generator with a squirrel-cage rotor and is connected to the grid through a transformer with star-triangle winding. The demand for reactive power from the WG is supplied by capacitors so as to reach a close-to-one power factor. The WG is modeled with blocks of an induction generator and a wind turbine available in the library of the simulation program and with parameters taken from the manufacturer data sheets [26,27]. The sub-transmission line is modeled by using lumped parameters. All loads are modeled by constant impedances and are grouped at bus 4 (Ld1: 0.3 MW and Ld2: 0.7 MW).

The DSTATCOM/FESS device proposed (maximum rated power: 100 kW and rated storage capacity: 750 Wh) is connected to the main bus (bus 3). The DC voltage of the DSTATCOM is 750 V and the capacitor used has a rated capacitance of 1000 μF. The DSTATCOM-VSI works with a switching frequency of 8 kHz whereas the Interface-VSI works with 20 kHz. The parameters of the FESS (PMSM and flywheel) are obtained from the manufacturer data sheets [13,18,19].

The major test system data are summarized in Appendix B while the DSTATCOM/FESS data in Appendix C.

The analysis and validation of the models and control algorithms proposed for the DSTATCOM/FESS controller are carried out through simple events that impose high demands upon the dynamic response of the device. Two cases are considered. The first case study (Case A) discusses the performance of the model and control algorithm of the device. For this, sudden variations in the active and reactive power references are imposed. The behaviour and the response of the device are observed with these requirements in mind. Moreover, an analysis is carried out of the efficiency of the PMSM in the whole speed variation range and for different powers. In the second case study (Case B), a test is made of the device proposed in the test system shown in Fig. 5. For this, a variation profile of wind speed is applied to the WG so that it makes

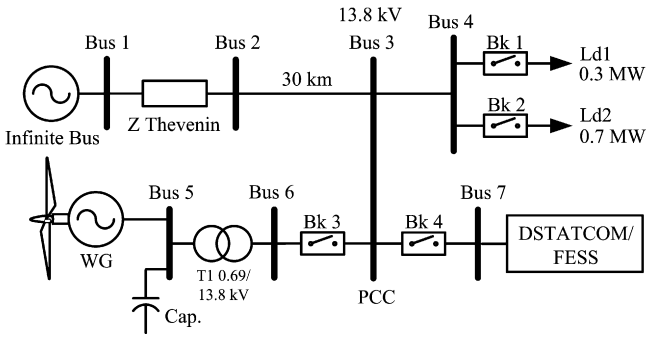

Fig. 5. Test power system.

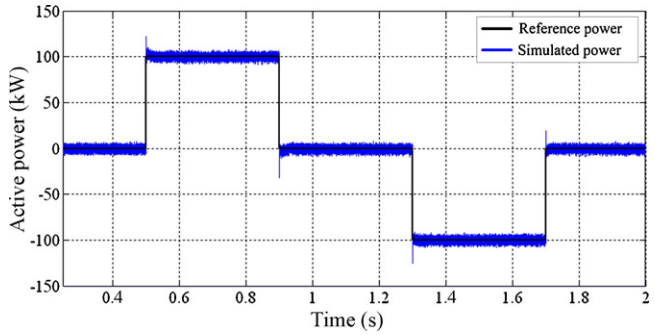

Fig. 6. Input/output active power of the DSTATCOM/FESS.

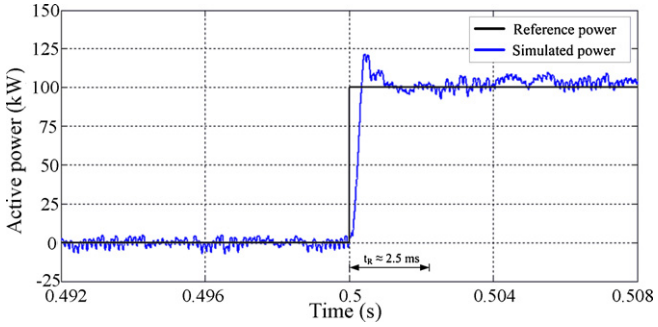

Fig. 7. Expanded scale of input/output active power of the DSTATCOM/FESS.

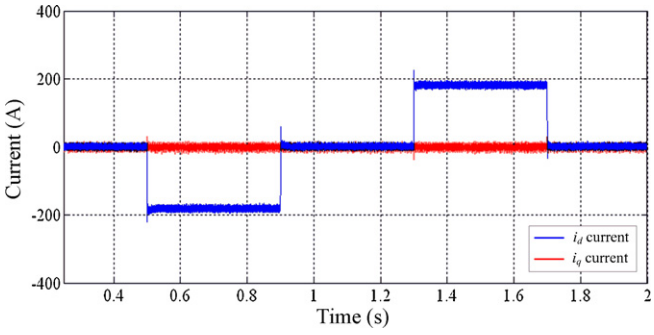

Fig. 9. DSTATCOM i_d and i_q currents.

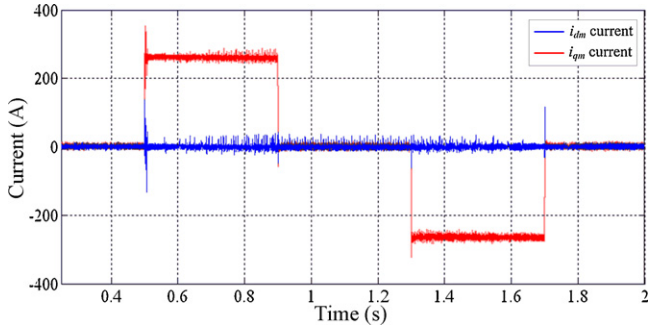

Fig. 10. PMSM i_{dm} and i_{qm} currents.

the DSTATCOM/FESS work in both ways, by storing and delivering energy. In addition, external perturbations are imposed, like a load variation, and the behaviour of the device in the different control modes is observed.

5. Simulation results

5.1. Case study A: DSTATCOM/FESS performance analysis

5.1.1. Variations of the active power reference

A positive and negative variation is applied in the active power reference P_r of the device and the reactive power reference is set equal to zero. The active power reference and the power generated by the device are shown in Fig. 6, and an expanded scale of these is shown in Fig. 7. In these figures it can be observed that the simulated power accurately follows the power reference, and it is also observed that the response time t_R of the device (time from $P=0$ to $P=P_{max}$) is around 2.5 ms. The DC voltage (U_d), which remains practically constant, is shown in Fig. 8. Only small variations of voltage are produced when the abrupt jumps of power take place. These voltage variations do not at any moment exceed 1% of the DC voltage.

The i_d and i_q currents of the DSTATCOM measured at the low voltage side of the transformer are shown in Fig. 9. An excellent decoupling can be observed among the currents, only a variation of the i_d current taking place under the requirement of the active power. In addition, the i_{dm} and i_{qm} currents of the PMSM are shown in Fig. 10. It is noted that under the power requirements imposed, only a variation of i_{qm} exists. In this way, the condition imposed on the control to keep i_{dm} equal to zero so as to obtain a maximum efficiency of the PMSM holds true.

5.1.2. Variations of the reactive power reference

In this case, a variation is applied in the reactive power reference of the device, and the active power reference is kept equal to zero. The DSTATCOM/FESS controller works as a DSTATCOM due to the fact that it does not have a requirement for active power. The reactive power reference and the reactive power generated by the device are shown in Fig. 11. In this figure, it can be observed that the simulated power accurately follows the power reference, and the inductive and capacitive reactive power required is delivered.

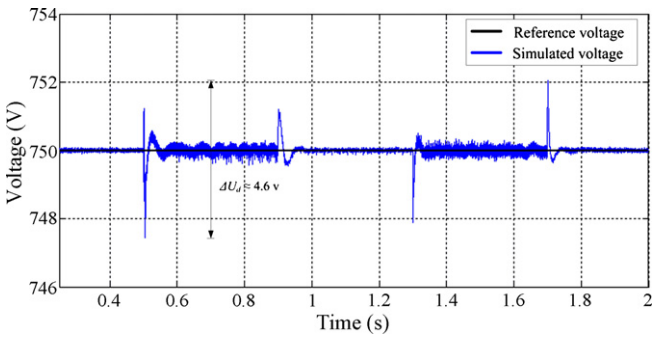

Fig. 8. Voltage at DC bus of the DSTATCOM/FESS.

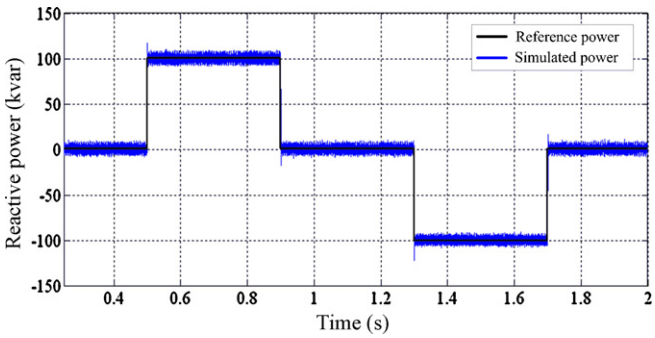

Fig. 11. Input/output reactive power of the DSTATCOM/FESS.

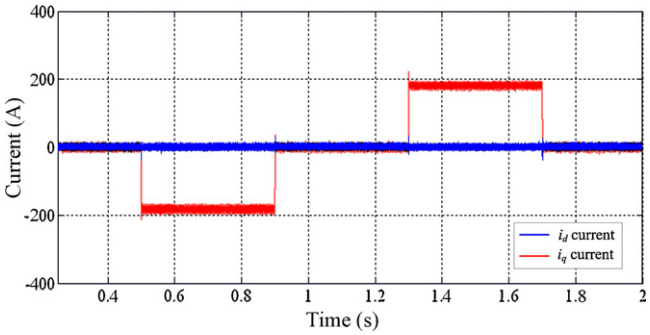

Fig. 12. DSTATCOM i_d and i_q currents.

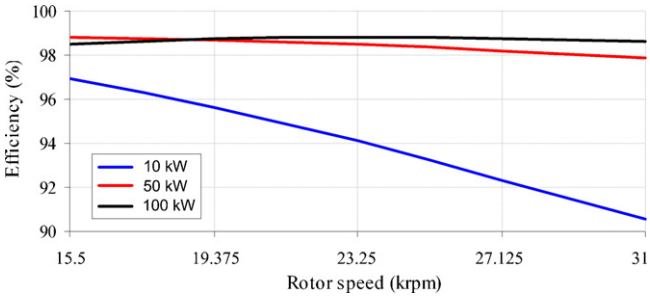

Fig. 13. Efficiency of the PMSM.

The i_d and i_q currents of the DSTATCOM are shown in Fig. 12. An excellent decoupling of the currents is again observed. With the requirement of reactive power, only the i_q current varies. The i_{dm} and i_{qm} currents and the torque of the PMSM are kept constant and close to zero. This is logically due to the fact that the system does not require active power.

5.1.3. Efficiency of the PMSM

Tests were made for different power requirements in the whole range of operation speeds of the machine. The results of the efficiency of the machine for an exchange of power of 10 kW, 50 kW and 100 kW are shown in Fig. 13. In this figure a high efficiency of the PMSM can be observed above 98% when the power is high (50% or 100% of the rated power), even in the whole speed range.

The main performance characteristics of these devices are summarized in Table 1. In this table, typical data specified in the manufacturer data sheets [13,18,19] are compared with the values obtained in the simulations carried out. It is observed that the values obtained from the models developed are quite well adjusted to the manufacturer data. In addition, it is noted that the implemented control allows the device to meet the demands required. The simulations showed an excellent adjustment between the reference values and those provided by the device. Furthermore, an excellent decoupling is kept in the control of the active and reactive power.

Table 1
Performance characteristics of the FESS.

Characteristics	Manufactures	Simulated
Response time	<5 ms	≈2.5 ms
Efficiency at rated power	98%	≈98.6%
Standby losses	<1.5% of rated power	0.3–1.1 kW 0.3–1.1% of rated power
Max DC ripple voltage	<1%	≈4.6 V ≈0.6%

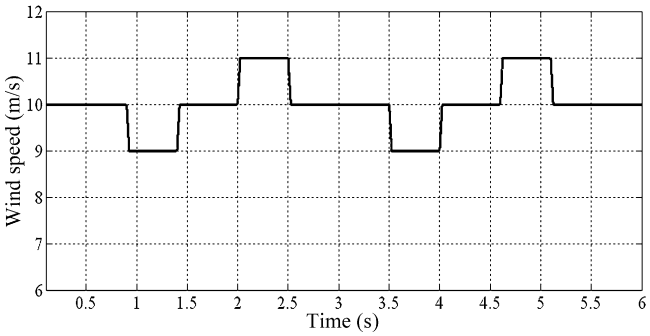

Fig. 14. Wind speed.

5.2. Case study B: DSTATCOM/FESS in the power system with wind generation

For this case, the basic system shown in Fig. 5 is used. A suitable profile for variation of the wind speed is applied, as shown in Fig. 14.

The wind speed variations cause significant fluctuations in the active and reactive power injected by the WG. The capacitor bank used with the WG is adjusted to compensate for the reactive power when the WG operates at a mean wind speed of 10 m/s. In bus 4, the load Ld1 = 0.3 MW is first connected (in $t = 0$ s) and then, in $t = 3$ s, the load Ld2 = 0.7 MW is added. The behaviour of the system is analyzed when the DSTATCOM/FESS is disconnected (Bk 4 opened) and connected (Bk 4 closed). The variations of active power injected by the WG-DSTATCOM/FESS system for both cases are shown in Fig. 15. With the DSTATCOM/FESS device connected, the variations of power from the WG are reduced and an active power that is practically constant is injected to the system.

For the reactive power control, three different cases are presented: DSTATCOM/FESS disconnected, DSTATCOM/FESS connected working in power factor control mode; and DSTATCOM/FESS connected working in voltage control mode.

The reactive power injected by the WG-DSTATCOM/FESS system is shown in Fig. 16. With the DSTATCOM/FESS connected working in PFCM, it is observed that the reactive power injected by the WG-DSTATCOM/FESS system is zero. Consequently, the device proposed has satisfactorily compensated for the reactive power variations of the WG. With the DSTATCOM/FESS connected working in VCM, the reactive power variations from the WG are compensated for and the device also generates or consumes the reactive power necessary to make the voltage in bus 4 be 1 pu.

The voltage at bus 4 is shown in Fig. 17. When there is no compensation, the voltage has significant variations due to both the power variations from the WG and those of the load. When the DSTATCOM/FESS device is connected in PFCM, there are no voltage variations due to wind power variations. However, this mode has the problem that the voltage has a value different from 1 pu and

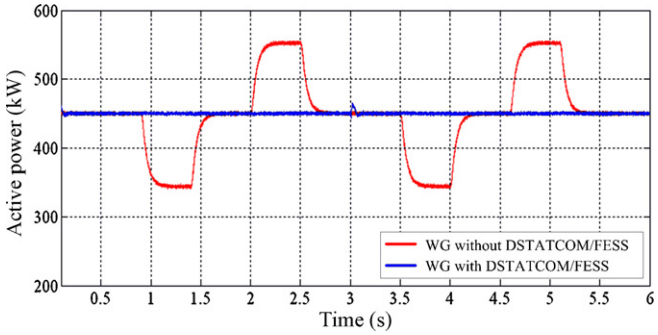

Fig. 15. Active power of the WG-DSTATCOM/FESS system.

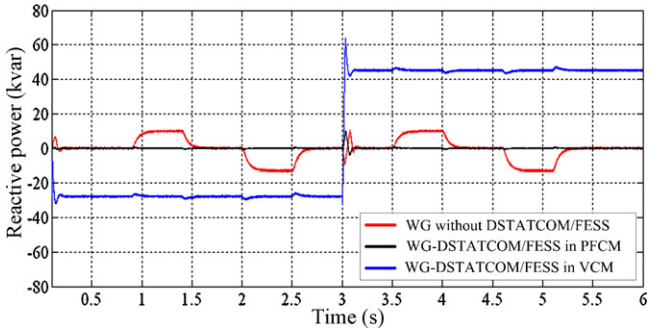

Fig. 16. Reactive power of the WG-DSTATCOM/FESS system.

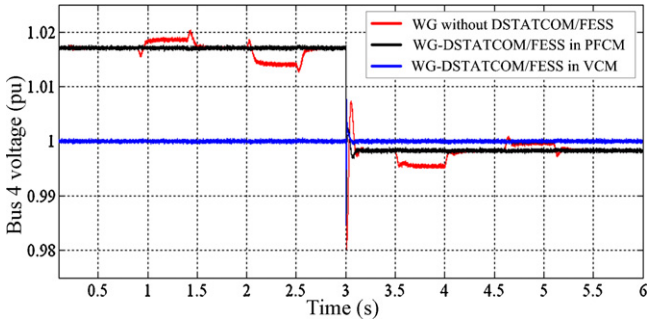

Fig. 17. Voltage at bus 4.

it varies with disturbances in the load. When the DSTATCOM/FESS device is connected in VCM, the voltage is maintained at 1 pu independently of the variations in wind power and variations of the load. This control mode solves in quite effective way the problem observed with the PFCM. Therefore, the VCM is the most convenient mode when the connection point of the WG does not have any other device that dynamically controls the voltage.

6. Conclusions

This paper presents model aspects and control algorithms of a DSTATCOM controller coupled with a High-Speed Flywheel Energy Storage System. A proposal is made of a detailed fully realistic model of the compensator and a novel multi-level control algorithm taking into account three control modes to mitigate problems introduced by wind power in power systems.

From the results obtained, it can be concluded that the detailed models and developed control algorithms have worked satisfactorily. The model proposed adjusts quite well to data from performance characteristics of true devices. With the control proposed, an excellent decoupling is kept in the control of active and reactive power.

Moreover, from the results it can also be concluded that with the device and control mode proposed, the power fluctuations coming from a WG are effectively compensated. Therefore, the insertion of wind power generation in power systems is improved. It was shown that the WG-DSTATCOM/FESS system can deliver a constant active power in a time range of seconds or more, depending on the storage capacity. For the reactive power control, it was shown that the system proposed is able to provide a unitary power factor or to obtain a dynamic control of the voltage in the connection point for power disturbances in the WG and also for fluctuations in the system such as sudden variations in the load.

Appendix A. List of symbols

a_t	voltage ratio of the coupling transformer
i_d, i_q	instantaneous currents of the DSTATCOM in dq reference frame
i_{dmr}, i_{qmr}	instantaneous currents of the PMSM in dq reference frame
J	moment of inertia of the flywheel
k_{inv}	constant of the VSI
L_t	equivalent leakage inductance of the coupling transformer of the DSTATCOM
m_a	modulation index
p	number of pairs of poles of the PMSM
P_{AC}	power of the AC side of the DSTATCOM
P_{Cu}	copper losses of the PMSM
P_{DC}	power of the DC side of the DSTATCOM
P_{Fe}	iron losses of the PMSM
P_{loss}	power losses of the PMSM
P_{mac_r}	power stored or delivered by the flywheel
P_{mec}	mechanical losses of the PMSM
P_r	reference power of the DSTATCOM/FESS
R_{pd}	loss resistance of the VSI
R_s	stator resistance of the PMSM
R_t	resistance of the coupling transformer of the DSTATCOM
T_{e_r}	electromagnetic torque of the PMSM
u	instantaneous voltage in the connection point of the DSTATCOM/FESS
u_{inv_d}, u_{inv_q}	instantaneous voltages of the DSTATCOM-VSI in dq reference frame
U_d	DC voltage of the DSTATCOM
x_1, x_2	control signals of the DSTATCOM-VSI
α	phase-shift between the converter output voltage and the grid AC voltage
ΔE	energy stored by the flywheel
ψ_m	magnetic flux of the PMSM
ω	electrical angular frequency
ω_m	angular speed of the PMSM
ω_{max}, ω_{min}	maximum and minimum operation speed of the flywheel
ω_{mr}	reference angular speed of the PMSM

Appendix B. Test system data

Line data are given in Table 2. Table 3 shows the transformer data. All pu quantities are on 13.8 kV and the transformer rated MVA base. Table 4 shows the main parameters of the generation unit coupled to the wind turbine. Table 5 shows the main parameters of the wind turbine and the power curve of the turbine is shown in Fig. 18. All pu quantities are on a 690 V and on the 750 kVA base. Finally, the most important load data are shown in Table 6.

Table 2
Line data.

ID	From bus	To bus	U_N (kV)	L (km)	R (Ω/km)	X (Ω/km)	B (μΩ^{-1}/km)
L1	2	3	13.8	30	0.01273	0.2933	4.0024

ID: component identifier; U_N: rated voltage; L: line length; and R, X and B: positive sequence resistance, reactance and susceptance of sub-transmission line.

Table 3
Transformer data.

ID	From bus	To bus	R (pu)	X (pu)	Rm (pu)	Xm (pu)	S_N (kVA)	N_p/N_s (kV/kV)
T1	5	6	0.002	0.021	500	500	1000	0.69/13.8

R and X: winding resistance and reactance; Rm and Xm: magnetization resistance and reactance; S_N: rated power; and N_p/N_s: voltage transformation ratio.

Table 4
Wind generator data.

ID	Bus	Machine	Rotor	S_N (kVA)	U_N (V)	Rs (pu)	Xs (pu)	Rr (pu)	Xr (pu)	H (s)	p
WG	5	Induction	Squirrel-cage	750	690	0.016	0.06	0.016	0.06	0.095	2

Rs and Xs: stator resistance and reactance; Rr and Xr: rotor resistance and reactance; H: inertia constant; and p: pairs of poles.

Table 5
Wind turbine data.

ID	H (s)	Wc-i (m/s)	Wc-o (m/s)	Wrp (m/s)
WT	2	4	25	16

Wc-i: cut-in wind speed; Wc-o: cut-out wind speed; and Wrp: rated wind speed.

Table 6
Load data.

ID	Bus	P_L (kW)	Q_L (kvar)
Ld1	4	300	0
Ld2	4	700	0

P_L and Q_L: load real and reactive power.

Table 7
FESS data.

General							
ID	P_{max} (kW)	E (Wh)	t_d (s)	S_{min} (krpm)	S_{max} (krpm)	J (kg m^2)	U_d (V)
FW	100	750	27	15.5	31	0.72	750

P_{max}: maximum rated real power; E: rated storage capacity; t_d: discharge time; S_{min} and S_{max}: minimum and maximum operation speed; J: polar inertia (PMSM + flywheel); and U_d: DC voltage.

Table 8
PMSM data.

PMSM				
Motor/generator	ψ_m (Wb)	L_d, L_q (μH)	R (mΩ)	p
Permanent magnet three-phase, synchronous	0.052	100	8	2

ψ_m: flux induced by magnet; L_d and L_q: d and q axes inductances; and R: resistance of the stator windings.

Appendix C. DSTATCOM/FESS controller data

Tables 7–9 summarize the most important data corresponding to the FESS, Interface and DSTATCOM subsystems.

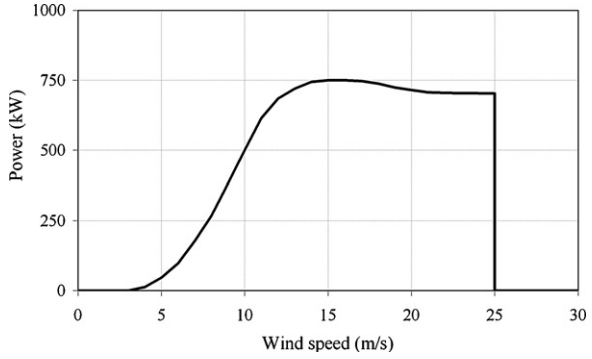

Fig. 18. Power curve of the wind turbine.

Table 9
VSI data of the Interface and the DSTATCOM.

T_f (μs)	T_t (μs)	U_f (V)	R_{on} (mΩ)	R_s (kΩ)
1	2	1	1	100

T_f: Current 10% fall time of the IGBT, T_t: current tail time of the IGBT; U_f: forward voltage for IGBT; R_{on}: internal resistance of the IGBT device; and R_s: snubber resistance.

References

[1] T. Ackermann, Wind Power in Power systems, John Wiley & Sons, London, UK, 2005.
[2] G.O. Suvire, P.E. Mercado, Impacts and alternatives to increase the penetration of wind power generation in power systems, in: X Symposium of Specialists in Electric Operational and Expansion Planning (SEPOPE), Florianopolis – Brasil, May 2006.
[3] G.O. Suvire, P.E. Mercado, Wind farm: dynamic model and impact on a weak power system, in: IEEE PES T&D LATINAMERICA, Bogotá – Colombia, August 2008.
[4] S.W. Mohod, M.V. Aware, Power quality issues & it's mitigation technique in wind energy generation, IEEE Harmonics and Quality of Power (September) (2008).
[5] J.C. Smith, M.R. Milligan, E.A. DeMeo, Utility wind integration and operating impact state of the art, IEEE Transaction on Power System 32 (August (3)) (2007) 900–907.
[6] R. Brad, J. McDowall, Commercial successes in power storage, IEEE Power & Energy Magazine (March/April) (2005) 24–30.
[7] J.M. Carrasco, Power electronic system for grid integration of renewable energy source: a survey, IEEE Transaction on Industrial Electronics 53 (August (4)) (2006) 1002–1014.
[8] J.P. Barton, D.G. Infield, Energy storage and its use with intermittent renewable energy, IEEE Transaction on Energy Conversion 19 (June (2)) (2004) 441–448.
[9] R. Hebner, J. Beno, A. Walls, Flywheel batteries come around again, IEEE Spectrum 39 (April (4)) (2002) 46–51.
[10] G.O. Suvire, P.E. Mercado, Utilización de Almacenadores de Energía para Mitigar los Problemas Introducidos por la Generación Eólica en el Sistema Eléctrico (Energy Storage Devices to Mitigate Problems Introduced by Wind Power Generation in Power System), XII Encuentro Regional Ibero-americano del CIGRÉ, Foz do Iguazú, Brazil, May 2007.
[11] Y.H. Song, A.T. Johns, Flexible AC Transmission Systems (FACTS), IEE Press, London, UK, 1999.
[12] R. de Andrade, G.G. Sotelo, A.C. Ferreira, L.G.B. Rolim, J.L. da Silva Neto, R.M. Stephan, W.I. Suemitsu, R. Nicolsky, Flywheel energy storage system description and tests, IEEE Transactions on Applied Superconductivity 17 (June (2)) (2007).
[13] Beacon Power website, www.beaconpower.com.
[14] T. Boutot, L. Chang, D. Luke, A low speed flywheel system for wind energy conversion, in: Proceedings of the 2002 IEEE Canadian Conference on Electrical & Computer Engineering, 0-7803-7514-9/02, 2002.
[15] R. Takahashi, L. Wu, T. Murata, J. Tamura, An application of flywheel energy storage system for wind energy conversion, in: International Conference on Power Electronics and Drives Systems, vol. 2, 2005, pp. 932–937.
[16] G. Cimuca, M.M. Radulescu, C. Saudemont, B. Robyns, Comparative study of flywheel energy storage systems associated to wind generators, in: Proceedings of the International Conference on Applied and Theoretical Electricity – ICATE 2004, Romania, October 2004.
[17] R. Cárdenas, R. Peña, G.M. Asher, J. Clare, R. Blasco-Giménez, Control strategies for power smoothing using a flywheel driven by a sensorless vector-controlled induction machine operating in a wide speed range, IEEE Transactions on Industrial Electronics 51 (June (3)) (2004).
[18] Flywheel Energy Systems website, www.magma.ca/~fesi.
[19] Urenco Power Technologies website, www.uptenergy.com.
[20] S. Samineni, B.K. Johnson, H.L. Hess, J.D. Law, Modeling and analysis of a flywheel energy storage system for voltage sag correction, IEEE Transactions on Industry Applications 42 (January/February) (2006) 42–52.

[21] H. Xie, S. Mei, Q. Lu, Design of a multi-level controller for FACTS devices, in: Proc. Power Systems and Communication Infrastructures for the Future, Pekín, China, September 2002.
[22] M.G. Molina, P.E. Mercado, Multilevel control of a Static Synchronous Compensator combined with a SMES coil for applications on Primary Frequency Control, in: Proc. CBA 2004, Gramado, Brazil, September 2004.
[23] B.K. Bose, Modern Power Electronics and AC Drives, Prentice Hall, USA, 2002.
[24] H. Toliyat, S. Talebi, P. McMullen, C. Huynh, A. Filatov, Advanced high-speed flywheel energy storage systems for pulsed power applications, IEEE Electric Ship Technologies Symposium (2005) 379–386.
[25] C. Mi, G.R. Slemon, R. Bonert, Modeling of iron losses of surface-mounted permanent magnet synchronous motors, IEEE (2001) 2585–2591.
[26] Neg Micon website, www.neg-micon.com.
[27] Ecotècnia website, www.ecotecnia.com.

G.O. Suvire was born in San Juan, Argentina, on November 13, 1977. He graduated as an electric engineer from the National University of San Juan (UNSJ), Argentina in 2002. He received his Ph.D. from the same University in 2009, carrying out part in the COPPE institute, in the Federal University of Rio de Janeiro in Brazil. His research interests include simulation methods, power systems dynamics and control, power electronics modeling and design, and the application of wind energy and energy storage in power systems.

P.E. Mercado (M′02, SM′02) was born in San Juan, Argentina, on August 26, 1953. He graduated as an electromechanical engineer from the UNSJ, and received his Ph.D. from the Aachen University of Technology, Germany. Dr. Mercado is currently a professor of electrical engineering at the UNSJ and a researcher with CONICET. He is a senior member of the IEEE Power Engineering Society. His research activities are focused on dynamic simulation, operation security, power electronics, economic operation and control of electric power systems.